Radiation cooling in laser-produced plasmas due to high-Z layers

J. C. Moreno, S. Goldsmith,* and H. R. Griem
Laboratory for Plasma Research, University of Maryland, College Park, Maryland 20742-3511

Leonard Cohen
Laboratory for Astronomy and Solar Physics, Goddard Space Flight Center, Greenbelt, Maryland 20771

R. Epstein, D. Bradley, P. A. Jaanimagi, and J. Knauer
Laboratory for Laser Energetics, University of Rochester, Rochester, New York 14623-1299
(Received 1 February 1989; revised manuscript received 22 May 1989)

Radiation cooling of laser-produced aluminum plasmas by highly ionized gold atoms was studied experimentally. The plasma was produced by irradiating 500-μm-diam glass spheres coated with two layers of aluminum and an intermediate gold layer of varying thickness. The 24-beam Omega laser system at a laser wavelength of 351 nm and intensity in the range $(2-3)\times 10^{14}$ W/cm^2 was used to produce the plasma. Electron temperatures were determined spectroscopically by measuring the $1s$-$2p$-to-$1s^2$-$1s2p$ line ratio in Al XIII and Al XII. With no gold layer the electron temperature of highly ionized aluminum is found to be close to 1400 eV. The introduction of a 0.01-μm layer of gold reduced the electron temperature to approximately 1100 eV, and with a 0.05-μm gold layer it was reduced to 700 eV. A gold layer also reduced the temperature of the sodium plasma produced from the glass as measured using Na X and Na XI line ratios. Time-resolved x-ray measurements showed additional evidence of cooling. Measurements of total x-ray emission and radiative energy calculations from a hydrodynamic code showed a 50% increase in radiated energy with the addition of 0.05-μm gold layer.

I. INTRODUCTION

The characteristic parameters of laser-produced plasmas such as electron temperature T_e, electron density N_e, and average ion charge $\bar{Z}$ depend on the laser parameters as well as on target geometry, structure, and material composition. T_e is related to the laser through the irradiation intensity I_L and its wavelength λ_L, increasing with I_L and with λ_L.[1] With spherical targets the radially flowing plasma is cooled by radiation and expansion. The radiation cooling rate L_r depends strongly on $\bar{Z}$, the effective nuclear charge of the ions, the local values of T_e and N_e, and radiation transport. As an example, the radiation cooling rates (per free electron per ion) of low-density and transparent plasmas (in coronal equilibrium) calculated by Post *et al.*[2] show that high-Z plasmas radiate considerably more than low-Z plasmas, with L_r increasing rapidly with Z. For $300 < T_e < 2000$ eV, the cooling rate for gold is larger by a factor of 100 than the aluminum cooling rate.

The subject of the present paper is a spectroscopic study of radiation cooling in plasmas produced by the interaction of a very intense laser with multilayered targets. Experimentally, the radiation cooling effect of high-Z ions is investigated through its effect on T_e. We utilized spherical glass targets coated with one or two layers of low-Z (Al) and a thin layer of high-Z (Au) materials. The line intensity ratio of the first resonance lines in H-like and He-like aluminum was studied as a function of the thickness ΔR_{Au} of the Au layer. T_e calculated from the line ratio decreased with ΔR_{Au} in reasonable agreement with hydrodynamic code calculations. An increase in the total x-ray emission was observed with increasing ΔR_{Au}. Hydrodynamic code calculations also provided a direct estimate of the energy fraction lost by radiation.

Our interest in the large L_r of high-Z ions arises from their possible use in inducing higher radiation cooling rates in low-Z plasmas. This might be achieved by introducing a relatively small amount of high-Z ions into the low-Z plasma. Relatively low-Z and medium-Z plasmas are considered as possible media for short-wavelength lasers. One of the established schemes to achieve population inversion, and possibly gain, at wavelengths below 200 Å is by three-body recombination into highly excited levels followed by cascades down to the ground-state level.[3-5] With the electron temperature decreasing rapidly enough so that the population of successive ionization states are not in equilibrium, and with sufficiently high density so that three-body recombination will overpopulate high quantum levels, population inversion may be attained. Some experimental evidence for the importance of radiative cooling by a high-Z plasma component in creating conditions for gain in the low-Z component is provided by the work of Seely *et al.*[4] Related theoretical modeling on the importance of cooling has been developed recently.[6,7]

II. EXPERIMENTAL ARRANGEMENT

The plasma was produced using the OMEGA 24-beam laser system at the Laboratory for Laser Energetics

TABLE I. Target and experimental parameters.

Target number	Al thickness (μm)	Au thickness (μm)	Target diameter (μm)	Pulse FWHM (ps)	Laser intensity (10^{14} W/cm^2)
1	1	0	516	650	2.5
2	1	0	498	700	3.1
3	1	0.01	510	675	2.1
4	1	0.01	502	650	2.9
5	1	0.05	513	705	2.3
6	1	0.15	495	650	1.9
7	1	0.15	502	705	2.5

(LLE) at the University of Rochester. Solid spherical glass targets, 500 μm in diameter, were coated either with a single 1-μm aluminum layer or with first a 0.5-μm aluminum layer, then a gold layer topped by another 0.5-μm aluminum layer. The width of the gold layer ΔR_{Au} is the variable parameter of the experiment. The laser intensity I_L, at a wavelength of 351 nm, was $(2\text{–}3)\times 10^{14}$ W/cm^2. On-target energy and absorbed energy were typically 1300 and 850 J, respectively. The shape of the laser pulse was close to a Gaussian with full width at half maximum (FWHM) of 670 ± 30 ps.

The primary experimental diagnostics included a 3-m grazing-incidence NASA spectrograph,[8] the MINIFLEX detector with four soft-x-ray diodes,[9] and the SPEAXS x-ray time-resolving spectrograph.[10] SPEAXS includes an elliptically curved PET crystal analyzer, used to disperse the x-ray spectrum (1.6–2.4 keV) onto the slit of an x-ray streak camera. A timing fiducial signal was generated by frequency quadrupling part of the main laser pulse obtained from mirror leakage and focusing it to a section of the photocathode consisting of a 0.02-μm layer of aluminum on mica.[11] The time resolution is 10 ps. Additional spectral data were obtained from the NASA grazing-incidence spectrograph containing a 1200 line/mm grating blazed at 2° 35′, employed at 88° incidence angle, giving a peak efficiency at 60 Å. Time-integrated spectra were recorded on 10-in.-long Kodak type 101-05 photographic plates, covering the spectral region between 6 to 70 Å. The characteristics of the laser and target parameters used in this experiment are given in Table I.

The spectra obtained by SPEAXS and by the grazing-incidence spectrograph were digitized by a Perkin-Elmer microdensitometer and stored on a disk for computer analysis. Line intensities were determined by fitting a Gaussian profile to the observed lines, after a proper subtraction of the continuum contribution. The energy radiated within a line is obtained by integration under the profile as a function of wavelength. The relative intensity calibration of the 101-05 plates was performed using the 2.2-m grazing-incidence spectrograph attached to a University of Maryland θ pinch. It is estimated that the error in the relative intensity calibration of the 101-05 plates is less than 10%.

III. EXPERIMENTAL RESULTS

The data presented here consist mostly of time-integrated spectra obtained with the grazing-incidence spectrograph and time-resolved spectra obtained with the SPEAXS spectrograph. Figure 1 shows a typical x-ray spectrum at the peak of the laser pulse for a target with aluminum and no gold. It is difficult to subtract out the background level from these x-ray lines due to the large continuum signal and broadline widths (due to instrumental resolution). In Fig. 2 we show the time dependence of Lyman series lines of Al XIII and Si XIV. The effect of adding an increasingly thick gold layer can be seen in these traces. The peak of the laser pulse is approximately at 0 nsec for these plots. Saturation of the streak camera is partly responsible for the flattening of the peak of the Al XIII Ly-α line in Fig. 2(a). All x-ray signals in these plots start with a delay relative to the laser signal, but there is no relative delay between their initial rise. This is because the initial part of the signal is

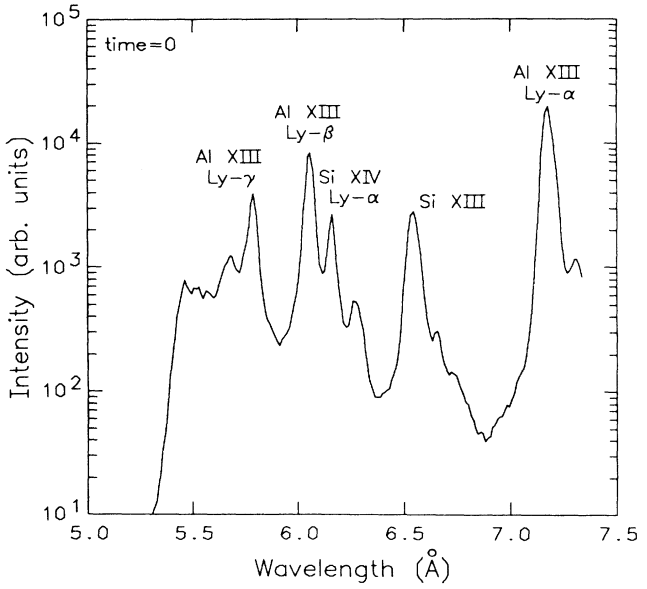

FIG. 1. X-ray spectrum of a target with Al on glass, at peak laser intensity.

mainly continuum emission as depicted by the dashed line in the plots.

While in Fig. 2(a) the target did not contain an intermediate gold layer, Figs. 2(b) to 2(d) show the effect of the gradual increase in the thickness of the gold layer on the Al XIII Ly-α, Ly-β, and Si XIV Ly-α signals. The presence of gold, even a 0.01-μm layer, causes a decrease in observed peak intensities and a faster decay rate in the emission intensity. Changes observed in the time histories for different targets and burnthrough analysis will be discussed in more detail in a later section.

The grazing-incidence spectra in the region 6 to 22 Å are presented in Fig. 3 for targets with 0, 0.01, and 0.05 μm of gold, respectively. Note how the background in-

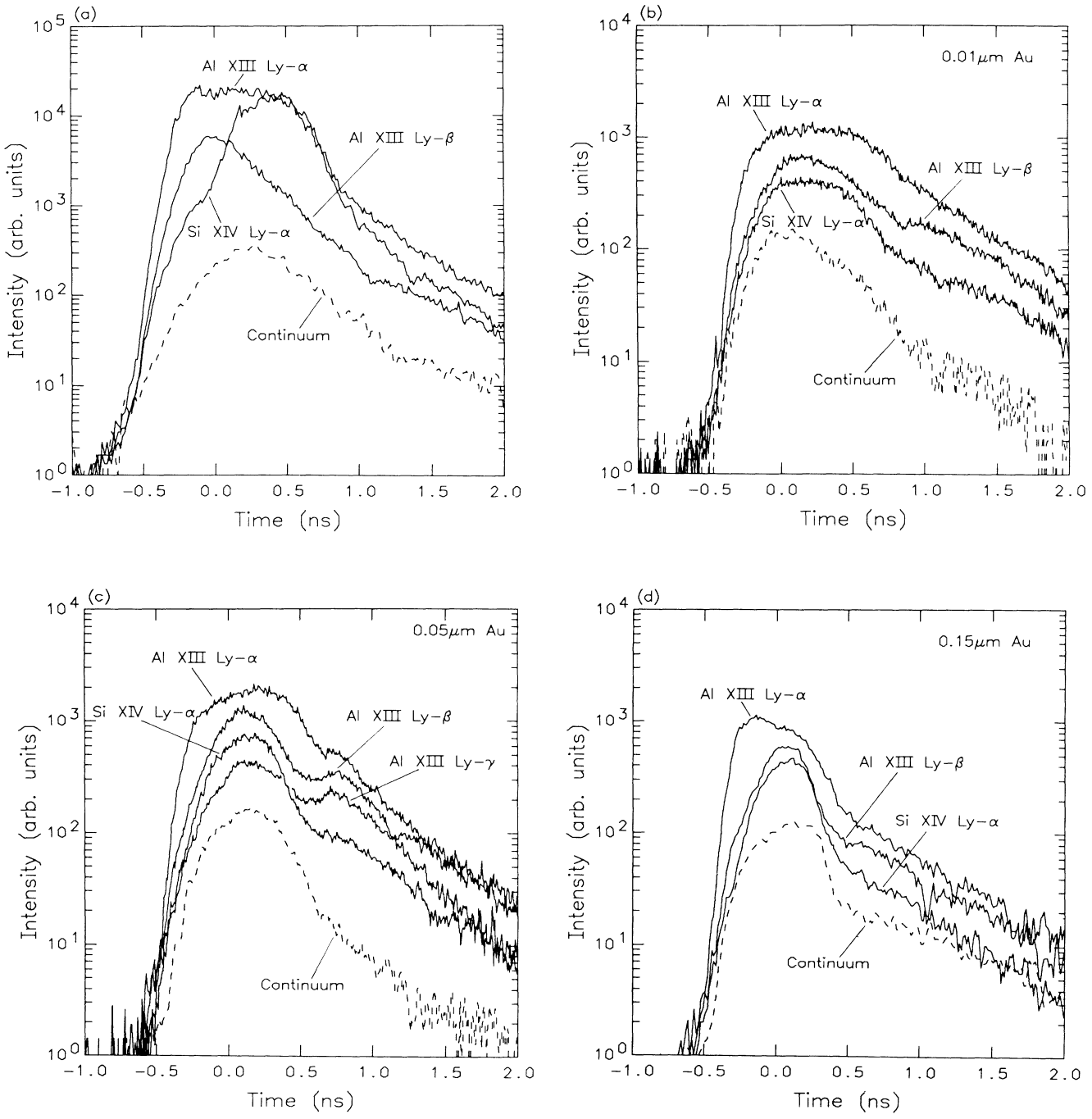

FIG. 2. Intensity of Al XIII and Si XIV Lyman series lines as a function of time for different Au layer thicknesses. The dashed line represents the time history of continuum emission. (a) Target with no Au layer. (b) Target with 0.01-μm Au layer. (c) Target with 0.05-μm Au layer. (d) Target with 0.15-μm Au layer.

creases significantly, as the gold thickness is increased, due to increased gold line and continuum emission. Targets which contained a 0.15-μm gold layer produced mainly a gold continuum spectrum in this region which overwhelmed the line emission. In general the main identified lines, in the xuv, for these targets are the Lyman series lines corresponding to the hydrogenic ions of aluminum, oxygen and sodium. In addition, the $1s^2\,{}^1S-1s2p\,{}^1P$ transitions in the He-like ions of these elements were observed, and in most cases Li-like lines of aluminum and silicon were also observed. Relative intensities of the hydrogen-like and helium-like lines can be used to determine T_e, and the effect of the presence of gold on T_e. The intensity ratio $1s$-$2p$-to-$1s^2$-$1s2p$ of H-like and He-like Al, Na, and O are presented in Fig. 4 as a function of ΔR_{Au}. This data clearly indicate that the increase in gold layer thickness leads to a decrease in the H-like Ly-α intensity relative to that of the He-like resonance line for Al and Na. Obviously, this is an integrated effect, both in time and space. In addition to the effect of the gold, plasma opacity should also influence the observation. These effects and others will be discussed in detail in Secs. IV and V to show the effective cooling of the aluminum plasma by the introduction of gold impurity.

IV. PLASMA PARAMETERS AND RADIATION COOLING

A. General considerations

The main goal of the present investigation was to study the enhancement of radiative cooling in laser-produced

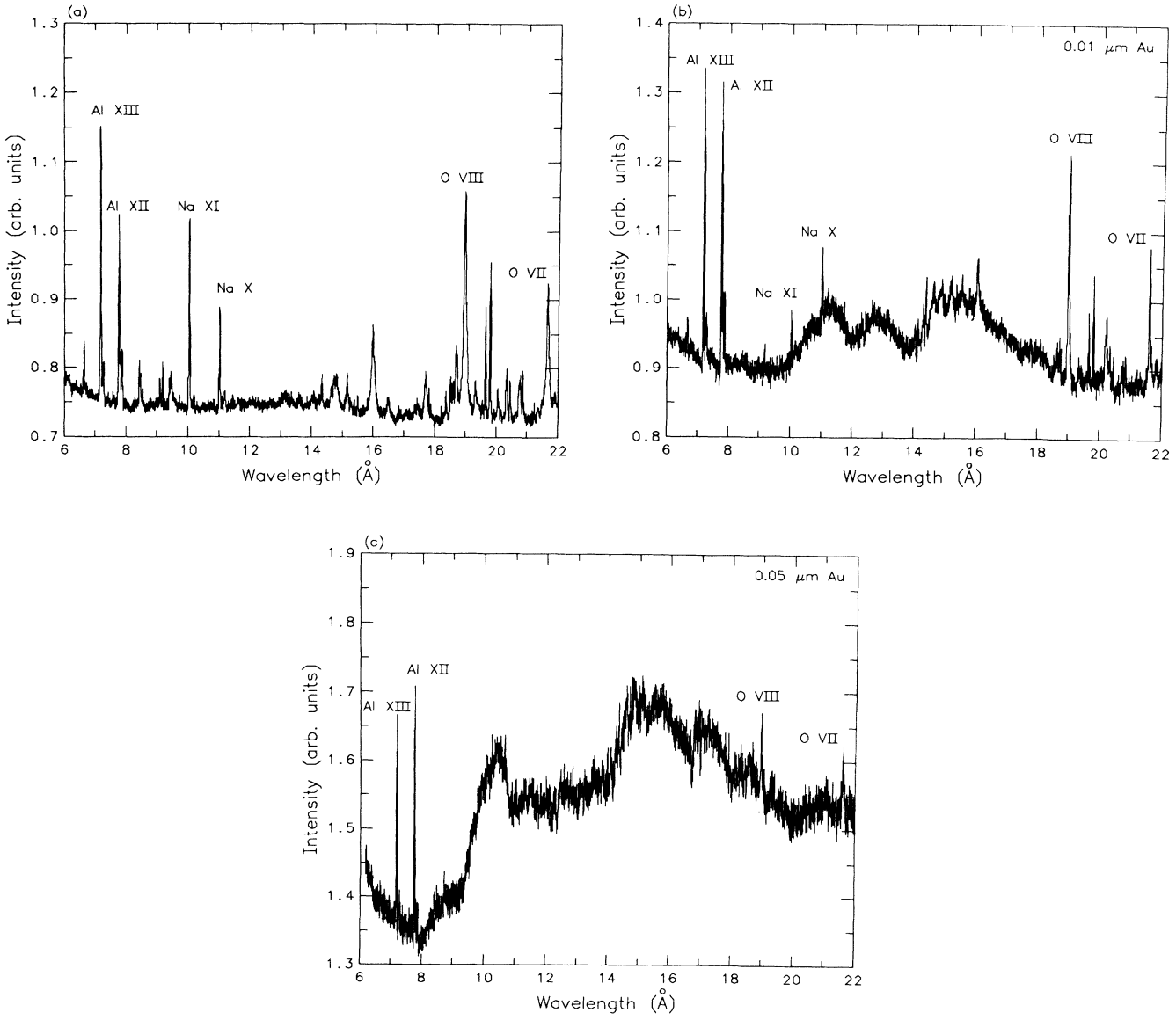

FIG. 3. Grazing-incidence spectra of targets with Al and varying Au layer thicknesses in the spectral range 6–22 Å. The resonance lines are indicated. (a) Target with no Au layer. (b) Target with 0.01-μm Au layer. (c) Target with 0.05-μm Au layer.

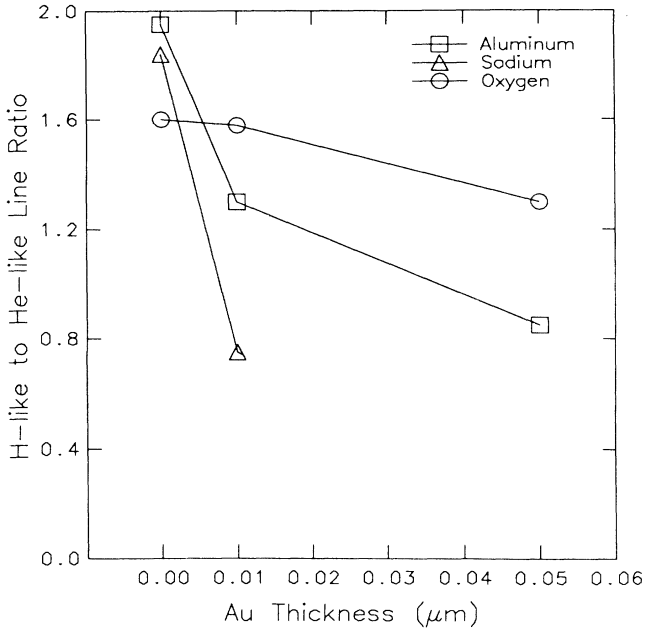

FIG. 4. Observed $1s$-$2p$–to–$1s^2$-$1s2p$ line ratios of Al, Na, and O as a function of gold layer thicknesses ΔR_{Au}.

plasmas resulting from the addition of small concentrations of high-Z ions. Line emission was produced in these plasmas by highly ionized aluminum ions ($\bar{Z}\sim 13$), gold ions ($\bar{Z}\sim 36$), oxygen ions ($\bar{Z}\sim 8$), silicon ions ($\bar{Z}\sim 14$), and traces of sodium and calcium ions (Na X, Na XI, Ca XVIII). Spectral line intensities were observed and used to determine T_e. The changes in the radiative energy rates are implied by the changes in T_e, as well as by measurements of total x-ray emission, and the interpretation is supported by additional code calculations of the plasma behavior.

The electron temperature of the laser-produced plasma is determined by a complex energy balance process, where the absorbed incoming laser energy is converted into internal plasma energy, ionic expansion kinetic energy, and radiative energy. With constant input energy, the local, instantaneous value of T_e will be determined to a large extent by the rate of radiative energy loss. It should be emphasized that in our experiment we interpret the relative changes of T_e, for the different targets, as valid indicators of the changes in the radiative loss, where a decrease of T_e indicates an increase in the radiative loss.

An important question is where in the plasma and at what point in time can T_e be determined? In spherical laser-produced plasmas T_e might change with time and is also a function of the radial position r_p. The electron temperature is lowest close to the solid target and increases toward the critical density layer at $r_p=R_c$. Beyond this layer there is a relatively slow decrease of T_e in the expanding plasma. The determination of T_e in spherical laser-produced plasmas, using plasma spectroscopy methods, gives some global measure for T_e weighted over the plasma region where the emission occurs. The values of T_e presented below are therefore an emissivity weighted average measure of T_e integrated over time. We will present first the values of average T_e and N_e, as obtained from observed line ratios, and discuss later the significance and implications of the results. Plasma parameters were also evaluated theoretically by means of a hydrodynamic code LILAC,[12] which as expected models the decrease in T_e.

B. Line ratio diagnostics modeling

Line ratio diagnostics generally use numerical model calculations of line ratios to determine the electron temperature. Several collisional-radiative (CR) models of highly ionized aluminum have been developed to analyze line intensities and line ratios.[13–16] We use the results of Duston and Davis,[16] which include the effects of radiation absorption, to analyze our experimental data for aluminum, as their ranges of T_e and N_e agree with the expected values for the present experimental conditions. Similar model calculations, but neglecting opacity, were performed here for sodium and oxygen ions to obtain T_e for plasmas containing these ions.[17]

Line ratios were calculated by Duston and Davis for T_e in the range 300 to 1800 eV, and calculated here assuming coronal equilibrium for T_e up to 10 keV. Although Duston and Davis ran their calculation as a function of ion density N_i, in the range 10^{18} to 10^{23} cm^{-3}, i.e., roughly equivalent to N_e in the range 10^{19} to 10^{24} cm^{-3}, we were mostly interested in N_e up to 9×10^{21} cm^{-3}, the critical density. A lower range for T_e is needed for the calculated line ratios in the sodium and oxygen plasmas. The source for the sodium ions is in the glass and the sodium line ratio therefore represents the effect of the heat flux after penetrating the outer metallic layers. The oxygen may originate from the glass and from oxide layers on the target surface.

C. Model values for T_e and N_e

Calculated ratios for $1s$-$2p$–to–$1s^2$-$1s2p$ lines in the H-like and He-like ions of aluminum, sodium, and oxygen as a function of T_e are presented in Fig. 5 from the results of a CR model neglecting opacity. For the case of aluminum a more detailed calculation, with opacity effects, is also included in the figure. Comparing these calculations to measured line ratios we obtain T_e as a function of the gold layer thickness ΔR_{Au} presented in Fig. 6. Error bars indicated for Al are representative of all the measurements. The principal factors that determine the measured T_e in the actual plasmas are the gold layer thickness, ionization energies of the emitting ions, and the heat flux. The dependence of T_e on Z is mainly due to the temperature region of the plasma at which these ions exist being dependent upon the ionization energy of the ions. The trend shown, a decrease in T_e as a function of ΔR_{Au}, suggests an increase in the energy loss. As this trend is already observed with $\Delta R_{\mathrm{Au}}=0.01$ μm, where only a small fraction of the laser input is used to produce the gold plasma, the increase in the radiative loss should be considerable. The average values of T_e in

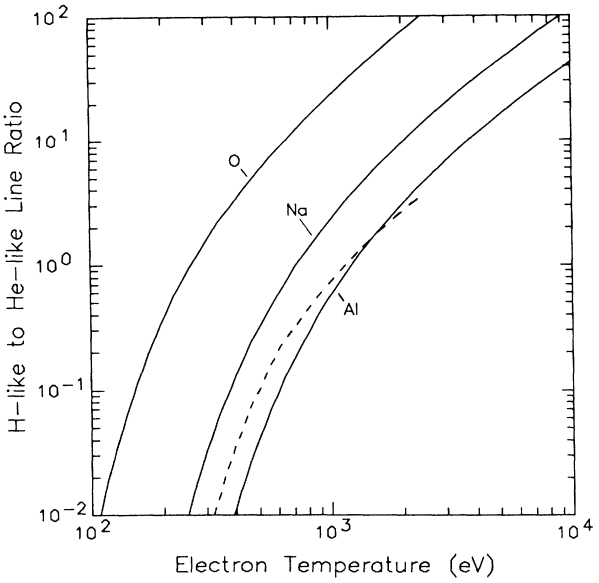

FIG. 5. Calculated $1s$-$2p$–to–$1s^2$-$1s2p$ line ratios of Al, Na, and O, assuming a CR model, as a function of T_e. The dashed line shows a CR calculation of the Al line ratio including opacity effects.

aluminum plasmas calculated by the hydrodynamic code LILAC, which included non-LTE effects, are also shown in Fig. 6. The variations seen there can be attributed in part to modeling assumptions, opacity effects and the radial location at which the temperature was obtained from LILAC. Opacity corrections act to decrease the measured values of T_e. It is the opacity corrected values of T_e for Al from the $1s$-$2p$–to–$1s^2$-$1s2p$ ratio, for an ion density of 10^{20} cm^{-3}, which are included in Fig. 6. For the temperature range which we study here, the opacity correction is approximately 10%. In addition, laser irradiation nonuniformity has been shown to be important in thermal transport analysis and may influence our measurement of T_e here.[18–20] It is significant, however, that the code and the experimental results agree well on the trend of the change in T_e.

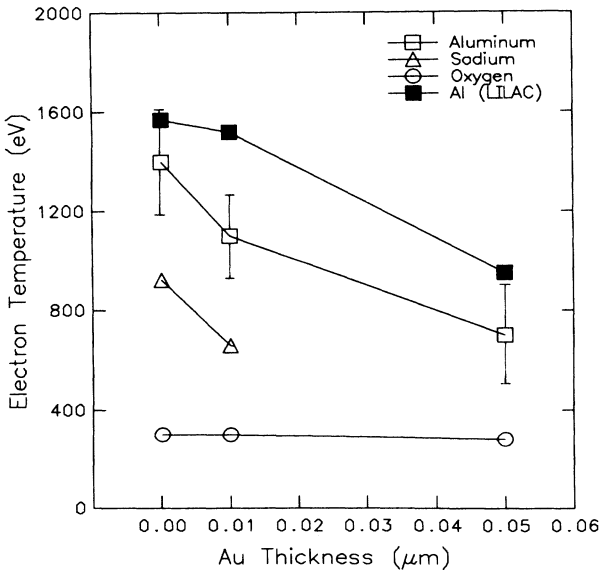

FIG. 6. Average T_e as a function of gold layer thickness. □, Al plasma (with absorption corrections). ■, LILAC calculations for Al plasma. △, sodium plasma. ○, oxygen plasma.

Significantly lower values for T_e are obtained when the spectra of ions of sodium and oxygen are used in the line ratio method. This is consistent with the measured line intensities being emissivity weighted and therefore being a measure of T_e averaged over the plasma region where these ions exist. Sodium, like aluminum, shows a decrease in temperature with gold thickness, while oxygen emission occurs from the same low-temperature plasma region in all cases with no decrease in intensity observed. The heat flux reaching the glass is less than that reaching the outer layers, which could reduce the electron temperature where the sodium (and possibly oxygen) originates.

A lower limit for the average N_e can be obtained if a density sensitive ratio is used to estimate average T_e. The results of Duston and Davis allow us to use two additional line ratios for this purpose, $1s^22p^2P-1s2p^2{}^2D$ to $1s^2$-$1s2p$ and $1s$-$2p$ to $1s^2$-$1s3p\,{}^1P$. Unfortunately, the last transition is obscured by a Si XIII line, and only the first one can be used. The line ratio $1s^22p^2P-1s2p^2{}^2D$ to $1s^2$-$1s2p$ is strongly affected by absorption, unlike the $1s$-$2p$ to $1s^2$-$1s2p$ transition ratio used previously. Using the measured values for T_e we find the condition $N_e \geq 10^{21}$ cm^{-3}, with opacity corrections included, for the two line ratios to be consistent.

D. Radiative energy losses

Radiative energy from the plasma calculated with the LILAC code and the measured total soft-x-ray emission are plotted in Fig. 7 for increasing gold thickness. Calibration of the x-ray diodes for total radiated energy has an error of approximately ±40%, but the relative error in the measurements is less than ±10%. Good agreement is observed between the two plots in Fig. 7 for the variation of radiated energy with ΔR_{Au}. This data demonstrate the marked increase in the radiative energy resulting from the introduction of 0.01 μm of gold into 1-μm aluminum. However, the further increase of ΔR_{Au} to 0.05 μm resulted in a smaller relative increase in radiated energy. The fraction of the radiated energy to the absorbed energy increased from 21% to 42% in going from no gold to a 0.05-μm thick layer of gold. Measured radiated energy saturated and even decreased slightly for layers thicker than 0.05 μm. These results are similar to a previous experiment performed on OMEGA in which x-ray conversion efficiencies of Au plasmas were measured as a function of Au thickness and laser intensity.[21] Solid CH targets coated with Au were used in the previous experiment and resulted in somewhat greater x-ray conversion efficiencies than measured in the present experiment.

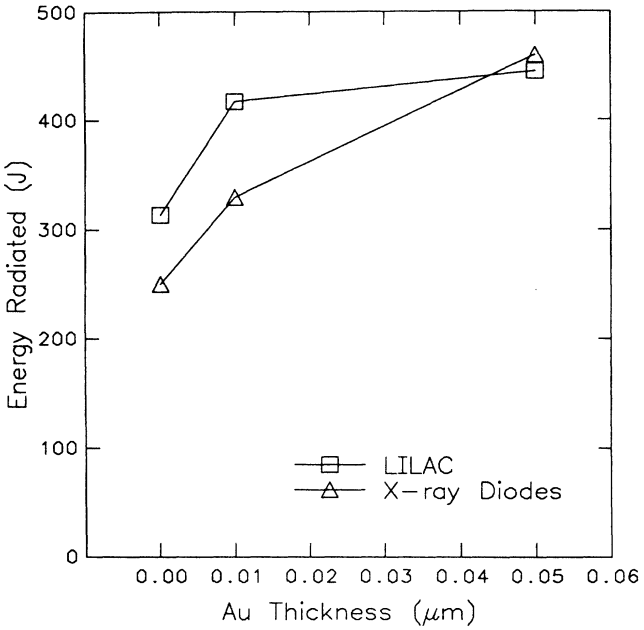

FIG. 7. Total energy radiated as a function of gold layer thickness from LILAC calculations and measurements of soft-x-ray emission using x-ray diodes.

V. DISCUSSION

An estimate of the effect of self-absorption on the line intensity ratio of the H-like and He-like resonance lines in the aluminum plasma is obtained from Fig. 12 in Ref. 15. The effect of absorption on the line ratio is calculated for two uniform and cylindrical aluminum plasmas with radii of 50 and 500 μm, which are optically thick. When T_e is smaller than 1100 eV, the neglect of absorption results in erroneously high estimates for T_e while if T_e is larger than 1100 eV the opposite effect occurs on neglecting the absorption. In the electron temperature region near 1100 eV the effect of absorption on the determination of T_e is negligible, if the resonance line ratio is used. According to the model of Duston and Davis, when the uncorrected initial values of T_e are in the range 1000–1500 eV, correcting the absorption effect is feasible even if the exact dimensions of the plasma are not known. Determination of T_e using this model is more difficult if it is also sensitive to the dimensions of the laser plasma, as is the case of the ratio $1s^2 2p\,^2P - 1s2p^2\,^2D$ to $1s^2$-$1s2p$ (Ref. 15, Fig. 11).

The burnthrough of the laser heat front can be determined from the data in Fig. 2. We have already indicated that at early times the SPEAXS spectra contain the contribution of continuum radiation in the spectral range 5–7 Å. Subtracting the estimated continuum background from the Si XIV Ly-α line in Fig. 2(a) we obtain a burnthrough time through 1 μm of aluminum of about 300 ps. The succeeding figures show x-ray time histories for targets with a gold layer inserted between 0.5-μm aluminum layers. In these cases the difference in time between the onset of the Al and Si line emission is $\sim$150 ps. Relating this value to a burnthrough time is not straightforward due to the complication of having two separate Al layers separated by a Au layer. However, the measured difference in time (150 ps) between Al and Si onset would indicate that most of the Al emission is from the inner 0.5-μm layer of Al. These results are also consistent with increased layer mixing due to the addition of a Au layer. Recent theoretical modeling predicts that mixing is a necessary condition for effective cooling.[7] The contribution of hydrodynamic mixing to the observed cooling is a subject that requires further investigation.

Effects of the gold layer are also noticeable in Fig. 2 on the later part of the x-ray line emission. Increasing the thickness of the gold layer resulted in a faster decay rate for the Al and Si line emission, indicative of radiation cooling from the gold seeding. In addition the Al XIII Ly-β and Ly-γ emission shows an increase in intensity about 700 ps after the peak of the laser pulse in Fig. 2(c). Since this "bump" in the time history is most evident in the higher members of the Al XIII Lyman series, and is not observed in silicon or continuum emission, it is most likely due to three-body recombination into higher n (quantum number) levels as the plasma rapidly cools. The 0.05-μm thick layer of gold seems to be the most effective in this case in radiatively cooling the plasma and possibly achieving a population inversion in higher-n levels of H-like Al.

VI. SUMMARY AND CONCLUSIONS

This paper reports the observation of enhanced radiation cooling of laser-produced aluminum plasmas by higher ionized gold. The plasma was produced by irradiating glass spheres typically coated with two layers of aluminum, each 0.5 μm thick, and a much thinner intermediate gold layer. Average electron temperatures were determined spectroscopically by measuring the $1s$-$2p$–to–$1s^2$-$1s2p$ transition ratio and using collisional-radiative models. The electron temperature was studied as function of the gold layer thickness. With no gold layers T_e of highly ionized aluminum was measured to be close to 1400 eV, a value consistent with the hydrodynamic code LILAC. The introduction of a 0.01-μm layer of gold reduced the measured value of T_e to approximately 1100 eV, and with 0.05 μm of gold T_e was reduced to 700 eV. The gold layer also affected T_e of the plasma produced from the glass spheres. The electron temperature determined by the same transition ratio in sodium decreased from 930 eV, with no gold seeding, to 670 eV with a 0.01-μm gold layer. A negligible effect on the temperature of oxygen ions from gold seeding was observed using the O VIII to O VII line ratio.

Measurements of total x-ray emission and comparisons to LILAC showed that with the 0.01- and 0.05-μm gold layers the radiative losses were 30% and 42% of the absorbed energy, respectively, while the radiation loss of the pure aluminum layer was 21% of the absorbed energy. Evidence for rapid cooling and recombination was ob-

served in the time history of the Al XIII Lyman series lines. In addition, time-resolved measurements of the x-ray spectral emission showed burnthrough of the heat front through aluminum layers to the glass. A burnthrough time of approximately 300 ps through 1 μm of aluminum was measured.

The results of this experiment are relevant both to target design for inertial confinement fusion, where the inclusion of high-Z layers is considered, and for the study of population inversion by three-body recombination into high atomic levels which depends on rapid cooling of the electrons.

ACKNOWLEDGMENTS

We thank the University of Rochester laser operations staff, experimental diagnostics staff, and target fabrication group for their outstanding support. We are grateful to W. E. Behring and U. Feldman for the use of the grazing-incidence spectrograph. The research and materials incorporated in this work were partially developed at the National Laser Users Facility at the University of Rochester's Laboratory for Laser Energetics, with financial support from the U.S. Department of Energy through Contract No. DE-AS08-87-DP-10684.

---

*Permanent address: School of Physics and Astronomy, Raymond and Beverly Sackler Faculty of Exact Sciences, Tel Aviv University, Tel Aviv 69978, Israel.

[1]C. E. Max, C. F. McKee, and W. C. Mead, Phys. Fluids **23**, 1620 (1980).

[2]D. E. Post, R. V. Jensen, C. B. Tarter, W. H. Grasberger, and W. A. Lokke, At. Data Nucl. Data Tables **20**, 397 (1977).

[3]S. Suckewer, C. H. Skinner, H. Milchberg, C. Keane, and D. Voorhees, Phys. Rev. Lett. **55**, 1735 (1985).

[4]J. F. Seely, C. M. Brown, U. Feldman, M. R. Richardson, B. Yaakobi, and W. E. Behring, Opt. Commun. **54**, 289 (1985).

[5]P. Jaegle, G. Jamelot, A. Carillon, A. Klisnick, A. Sureau, and H. Guennou, J. Opt. Soc. Am. B **4**, 563 (1987).

[6]C. H. Nam, E. Valeo, S. Suckewer, and U. Feldman, J. Opt. Soc. Am. B **3**, 1199 (1986).

[7]R. Epstein, Phys. Fluids B **1**, 214 (1989).

[8]W. E. Behring, R. J. Ugianski, and U. Feldman, Appl. Opt. **12**, 528 (1973).

[9]G. Pien, M. C. Richardson, P. D. Goldstone, R. H. Day, F. Ameduri, and G. Eden, Nucl. Instrum. Methods B **18**, 101 (1986).

[10]B. L. Henke and P. A. Jaanimagi, Rev. Sci. Instrum. **56**, 1537 (1985).

[11]P. A. Jaanimagi, L. DaSilva, G. G. Gregory, C. Hestdalen, C. D. Kiikka, R. Kotmel, and M. C. Richardson, Rev. Sci. Instrum. **57**, 2189 (1986).

[12]LILAC, LLE Reports No. 16 (1973) and No. 36 (1976) (unpublished).

[13]R. K. Landshoff and J. D. Perez, Phys. Rev. A **13**, 1619 (1976).

[14]J. D. Kilkenny, R. W. Lee, M. H. Key, and J. G. Lunney, Phys. Rev. A **22**, 2746 (1980).

[15]D. Salzmann and A. Krumbein, J. Appl. Phys. **49**, 3229 (1978).

[16]D. Duston and J. Davis, Phys. Rev. A **5**, 1664 (1980).

[17]J. C. Moreno, S. Goldsmith, and H. R. Griem, J. Appl. Phys. **65**, 1460 (1989).

[18]P. A. Jaanimagi, J. Delettrez, B. L. Henke, and M. C. Richardson, Phys. Rev. A **34**, 1322 (1986).

[19]J. Delettrez, R. Epstein, M. C. Richardson, P. A. Jaanimagi, and B. L. Henke, Phys. Rev. A **36**, 3926 (1987).

[20]J. C. Moreno, H. R. Griem, S. Goldsmith, A. Krumbein, R. Epstein, P. A. Jaanimagi, M. C. Richardson, and B. Yaakaboi, J. Appl. Phys. **63**, 674 (1988).

[21]P. D. Goldstone, S. R. Goldman, W. C. Mead, J. A. Cobble, G. Stradling, R. H. Day, A. Hauer, M. C. Richardson, R. S. Majoribanks, P. A. Jaanimagi, R. L. Keck, F. J. Marshall, W. Seka, O. Barnouin, B. Yaakobi, and S. A. Letzring, Phys. Rev. Lett. **59**, 56 (1987).